OFFICE OF NAVAL RESEARCH

Contract N00014-87-K-0494

R&T Code 400X027YIP

Technical Report No. 3

Phase Detection Interferometric Microscopy of Electrode Surfaces. Measurement of Localized Dissolution of Iron Electrodes.

by

H. J. Kragt, D. J. Earl, J. D. Norton, and H. S. White

Prepared for Publication in the

Journal of Electrochemical Society
(in press)

University of Minnesota
Department of Chemical Engineering and Materials Science
Minneapolis, MN 55455

Dec. 5, 1988

SECURITY CLASSIFICATION OF THIS PAGE

REPORT DOCUMENTATION PAGE

1a. REPORT SECURITY CLASSIFICATION **Unclassified**	1b. RESTRICTIVE MARKINGS
2a. SECURITY CLASSIFICATION AUTHORITY	3. DISTRIBUTION/AVAILABILITY OF REPORT
2b. DECLASSIFICATION/DOWNGRADING SCHEDULE	**Unclassified/Unlimited**
4. PERFORMING ORGANIZATION REPORT NUMBER(S) **ONR Technical Report 3**	5. MONITORING ORGANIZATION REPORT NUMBER(S)
6a. NAME OF PERFORMING ORGANIZATION **Dept of Chemical Engineering and Materials Science** 6b. OFFICE SYMBOL (If applicable) **Code 1113**	7a. NAME OF MONITORING ORGANIZATION **Office of Naval Research**
6c. ADDRESS (City, State, and ZIP Code) **University of Minnesota Minneapolis, MN 55455**	7b. ADDRESS (City, State, and ZIP Code) **800 North Quincy Street Arlington, VA 22217**
8a. NAME OF FUNDING/SPONSORING ORGANIZATION **Office of Naval Research** 8b. OFFICE SYMBOL (If applicable)	9. PROCUREMENT INSTRUMENT IDENTIFICATION NUMBER **Contract No. N00014-87-K-0494**
8c. ADDRESS (City, State, and ZIP Code) **800 North Quincy Street Arlington, VA 22217-5000**	10. SOURCE OF FUNDING NUMBERS PROGRAM ELEMENT NO. / PROJECT NO. / TASK NO. / WORK UNIT ACCESSION NO.

11. TITLE (Include Security Classification)
Phase Detection Interferometric Microscopy of Electrode Surfaces. Measurement of Localized Dissolution of Iron Microelectrodes.

12. PERSONAL AUTHOR(S)
Harlan J. Kragt, David J. Earl, John D. Norton, and Henry S. White

13a. TYPE OF REPORT	13b. TIME COVERED	14. DATE OF REPORT (Year, Month, Day)	15. PAGE COUNT
Technical	FROM _____ TO _____	**December 6, 1988**	**15**

16. SUPPLEMENTARY NOTATION

17. COSATI CODES			18. SUBJECT TERMS (Continue on reverse if necessary and identify by block number)
FIELD	GROUP	SUB-GROUP	**Fe microelectrode; high-resolution imaging; corrosion.**

19. ABSTRACT (Continue on reverse if necessary and identify by block number)

Phase detection interferometric microscopy (PDIM) was used to obtain high resolution surface images of 100 μm diameter Fe disk exposed to 0.1M H_2SO_4. The initiation and growth of corrosion pits at short time (0-30 sec) were observed on relatively smooth regions of the Fe surface (r.m.s. surface roughness ≅ 5.5 nm). The growth of pits at open circuit was measured with 1 nm resolution from the time of initiation to depths of 50 nm. The rate of vertical pit growth from PDIM analysis is characterized by the rate equation, $y = 0.15\ t_n^2$, where y is the pit depth (NM) and t is time (s). The topography of the Fe surface surrounding the pits remained virtually unchanged during pit growth, suggesting the presence of microscopic galvanic cells on the electrode surface.

20. DISTRIBUTION/AVAILABILITY OF ABSTRACT	21. ABSTRACT SECURITY CLASSIFICATION
☒ UNCLASSIFIED/UNLIMITED ☐ SAME AS RPT ☐ DTIC USERS	**Unclassified**
22a. NAME OF RESPONSIBLE INDIVIDUAL **Henry S. White**	22b. TELEPHONE (Include Area Code) **(612) 625-6995** / 22c. OFFICE SYMBOL

DD FORM 1473, 84 MAR — 83 APR edition may be used until exhausted. All other editions are obsolete.

SECURITY CLASSIFICATION OF THIS PAGE

Phase Detection Interferometric Microscopy of Electrode Surfaces. Measurement of Localized Dissolution of Iron Microelectrodes.

Harlan J. Kragt, David J. Earl, John D. Norton, and Henry S. White*
Department of Chemical Engineering and Materials Science
University of Minnesota
Minneapolis, MN 55455

Abstract. Phase detection interferometric microscopy (PDIM) was used to obtain high resolution surface images of a 100 μm diameter Fe disk exposed to 0.1M H_2SO_4. The initiation and growth of corrosion pits at short times (0-30 sec) were observed on relatively smooth regions of the Fe surface (r.m.s. surface roughness ≈ 5.5 nm). The growth of pits at open circuit was measured with 1 nm resolution from the time of initiation to depths of 50 nm. The rate of vertical pit growth from PDIM analysis is characterized by the rate equation, $y = 0.15\ t^2$, where y is the pit depth (nm) and t is time (s). The topography of the Fe surface surrounding the pits remained virtually unchanged during pit growth, suggesting the presence of microscopic galvanic cells on the electrode surface.

* Electrochemical Society Active Member.

Introduction. Time varying microtopographical features on electrode surfaces often play an important role in determining the behavior of electrochemical systems. A classic example of this is the dissolution and pitting of metal and metal alloys. Although the susceptibility of metals and alloys to corrosion pitting has obvious technological importance, direct experimental evidence of pitting mechanisms still remains elusive. It is widely accepted that the growth on an individual pit at open-circuit is the result of a localized galvanic cell operating on the specimen surface with the bottom of the pit preferentially dissolving with respect to the outer surface. The details of this phenomena remain unclear. For instance, little quantitative experimental data exist relating the point of initiation of a single pit to the initial physical and chemical properties of the substrate surface. Also, it is not clear to what extent local galvanic cells exist prior to pit initiation or how they develop across the surface during the early growth of the pit. These questions are difficult to address experimentally due to the microscopic scale on which pitting occurs and to the fact that the cathodic and anodic reactions are, to some extent, spatially separated across the electrode surface.

In this report, we describe, using phase-detection interferometric microscopy (PDIM), surface imaging of pits and the surrounding surface topography of 100 μm diameter Fe microelectrodes during the early stages of pit growth. PDIM is based on a non-contacting optical interferometric method[1,2,3] (see Experimental) that can rapidly image both conducting and non-conducting substrates, either in air, or submerged under thick electrolyte layers (up to 4 mm)[4]. Ultra-high vertical resolution (0.6 nm), submicron lateral resolution, and a large field of view make PDIM well suited for studying time varying microtopography of electrode substrates including, in particular, various forms of localized corrosion. We describe, herein, preliminary measurements of pit initiation and early growth on Fe in 0.1 M H_2SO_4. The focus of these preliminary measurements is on (1) topographical features that may lead to pit initiation, (2) growth kinetics in the early stages

of pit growth, and (3) structural changes of the area surrounding individual pits that provide clues to the formation of local galvanic cells.

Experimental. *Phase Detection Interferometric Microscopy.* A ZYGO (Middlefield, CT) Maxim 3D Laser Interferometric Microscope, hereafter referred to as a phase-detection interferometric microscope (PDIM), was used to image the Fe electrode surface. A detailed description of the microscope and measurement theory is given elsewhere[5]. A schematic diagram of the key components of the instrument are shown in Fig. 1. Topographical features of the electrode surface are measured by the microscope using optical phase measurement interferometry. Essentially, the PDIM consists of a Fizeau interferometer attached beneath the objective of an optical microscope. Light emitted by a 1mW He/Ne laser passes through a rotating disk diffuser, reflects off a polarizing beamsplitter, and is recollimated by the microscope objective. The light passes through a quarter wavelength retardation plate and illuminates the test surface. The bottom of the retardation plate is coated with a partially reflecting film which acts as the reference surface and the beam splitter for the interferometric analysis. Reflected light from the electrode and reference surfaces interfere, and the resulting spatially resolved intensities are recorded on a 244 x 388 pixel charge injection device (CID) array camera. The digitized output from the CID camera is analyzed to produce a phase map representing the relative differences in height between the reference and test surfaces. A video monitor connected to the array camera provides a direct optical image of the sample.

The microscope uses a dynamic phase measurement technique to determine the vertical surface heights. The intensity of light, I, detected by the CID array camera for position (x,y) is given by

$$I = I_1 + I_2\cos[\phi(x,y) + \alpha(t)].$$

I_1 represents the time averaged sum of reflected intensities from the reference and electrode surface. The second term on the right-hand side represents a time varying component of the interference intensity, where $\phi(x,y)$ is the initial phase difference between reflected wavefronts originating at the electrode and reference surfaces. To measure the vertical heights across the surface, 90° phase shifts are introduced between the reference and test signals using a piezoelectric transducer to move the reference surface at a constant rate towards the electrode surface. The intensity detected at each pixel of the camera is integrated during this movement and recorded after phase-changes of $\alpha(t) = 90, 180, 270, 360$, and 450° between reference and test signals. Integration of the interference intensity over these 5 intervals yield 5 values

$$A(x,y) = I_1' + I_2'[\cos\phi(x,y) - \sin\phi(x,y)]$$

$$B(x,y) = I_1' - I_2'[\cos\phi(x,y) + \sin\phi(x,y)]$$

$$C(x,y) = I_1' - I_2'[\cos\phi(x,y) - \sin\phi(x,y)]$$

$$D(x,y) = I_1' + I_2'[\cos\phi(x,y) + \sin\phi(x,y)]$$

$$E(x,y) = I_1' + I_2'[\cos\phi(x,y) - \sin\phi(x,y)]$$

from which the initial spatially dependent phase $\phi(x,y)$ is calculated[5] :

$$\phi(x,y) = \tan^{-1}\left[\frac{(A(x,y) + E(x,y) - 2C(x,y))}{2(B(x,y) - D(x,y))}\right] + \frac{\pi}{4}$$

The vertical heights across the electrode surface are computed directly from the phase measurement using the equation

$$h(x,y) = (\lambda/4\pi)\phi(x,y)$$

where λ is the wavelength of the illumination, (632.8 nm).

The vertical resolution of the microscope is limited primarily by stray vibrations and is specified by the manufacturer to be 0.6 nm. In our laboratory, we routinely measure calibrated vertical steps on metal films as small as 4 nm. The results described in this report focus on structures in the 5-80 nm range; these are well above the resolution of the microscope.

Fe Electrodes and Imaging Procedure. Fe disk electrodes were constructed by sealing 100 um wire (Alfa) in a glass pipette with epoxy resin (Mager, Sci.). Electrodes were wet sanded with 180, 600, and 4000 grit sandpaper, followed by polishing with 0.3 and 0.05 um alumina.

PDIM images of the Fe electrode surface were recorded in air following each of a series of six, 5s immersions of the electrode in 0.1 M H_2SO_4 contained in an open beaker. Prior to each imaging, the electrode was immersed for 5 s, removed and quickly transferred to a larger volume of distilled H_2O to remove the acid solution from the electrode surface. The electrode was further washed with distilled H_2O, dried, and placed under the microscope objective for imaging.

Imaging of surface topography after transfer from the solution required location of the same surface region for analysis. This was accomplished by using two 0.05 um alumina grains, which had adhered to the surface during polishing, as reference points to locate specific surface areas. The alumina grains also served as internal calibration of the vertical height measurements. Data acquisition and computer analysis of vertical heights using manufacturer provided software required approximately 30 s per sample.

Results and Discussion. The electrochemical behavior of the 100 μm Fe disk in 0.1 M H_2SO_4 exposed to air is shown in Fig. 2. Voltammograms observed on the microdisk are

qualitatively similar to that of macroscopic Fe electrodes, exhibiting potential regions of active, passive, and transpassive behavior. This general behavior is observed for Fe electrodes with diameters as small as 1 μm[6], although the dissolution current density is enhanced at the smaller wires (< 50 μm) due to quasi-radial transport of Fe^{2+} away from the electrode surface[7].

PDIM images of 100 μm diameter electrodes were recorded following immersion of the electrode at open circuit in 0.1 M H_2SO_4 contained in an open beaker. The open-circuit potential of Fe in this solution is -0.575 V vs SCE. At this potential, the Fe surface is dissolving at a rate controlled by the kinetics of hydrogen evolution and Fe dissolution. Purging the solution with N_2 to remove O_2 has an insignificant effect on the observed voltammetric response.

A low magnification image of the polished electrode surface in air is shown in Fig. 3. As seen in this image, the Fe wire protrudes slightly after polishing from the epoxy surface, a result of the difference in hardness of these materials. The vertical scale is highly exaggerated in this image, a feature common to all PDIM images shown below. The highest point on the electrode surface, relative to the epoxy plane, is ca. 1 μm. The electrode diameter is measured to be 105 ± 2 μm, in accordance with manufacturer's specifications.

Scanning the potential of the electrode within the active corrosion region (-0.5 to 0.15 V vs. SCE) results in rapid dissolution of Fe and recession of the wire into the epoxy. When the electrode is held at open-circuit, the dissolution process occurs at a much slower rate and is characterized by the formation of shallow microscopic pits randomly spaced across the electrode surface. Fig. 4, for instance, shows the initiation and growth of 2 pits spaced approximately 3 μm apart as a function of the time immersed in 0.1 M H_2SO_4. These same pits were observed on the video monitor. The images in Fig 4. are displayed at higher lateral magnification than the image of the entire electrode in Fig. 3 and show nanoscopic topographical features. The relative vertical dimensions have been inverted to

show the time evolution of pit growth (i.e., hills represent valleys and vice versa). As observed in the images, two small pits are observed following the initial 5 sec immersion of the Fe disk in 0.1 M H_2SO_4 which have heights of ca. 10 nm. Re-immersion of the electrode into the acid results in continued growth of these pits, as shown in the bottom two frames of Fig. 4. The images of Fig. 4 are representative of a number of pits observed across the electrode surface. However, not all of the pits observed during the 30 s interval initiated upon the first immersion in the acid solution. Furthermore, we occasionally witnessed the disappearance of pits between immersions. These pits did not reappear following subsequent reimmersion.

In general, the initiation of the pit was followed by parabolic vertical growth. Figs. 5 and 6 show line profiles across regions of the Fe microdisk surface that cut across 3 pits. The profile of the single pit in Fig. 6 corresponds to the pit marked by the arrow in Fig. 4. From PDIM measurement of the pit depth, y(nm), as a function of time(sec), the initial growth rate is given by $y \approx 0.15\ t^2$. Undoubtedly, this rate is affected by the immersion/drying procedure used to obtain images. Construction of a cell to allow in-situ imaging of the microelectrode is being pursued.

The appearance and growth of isolated corrosion pits suggest the formation of microscopic local galvanic cells on the electrode surface. A similar mechanism is often presented in describing pitting corrosion on metals held within the passive region (Fig. 2) in near neutral pH solutions. Under these conditions, O_2 reduction on the passivated surface, exterior to the pit, corresponds to the cathodic reaction. In the present study, the low pH would likely preclude the formation of a passive layer on the surface. Inspection of PDIM images of the area surrounding the pit show that these regions retain topographical features initially present on the surface. In Fig. 4, the inverted images of the surface prior to and after the initial immersion are essentially identical except for the initial growth of the two isolated pits. Although slow uniform dissolution of the metal

surrounding the pit might lead to time-varying features not resolved by PDIM, it is readily apparent that the rate of metal dissolution is largest at the two localized areas.

Conclusion. PDIM imaging of Fe microelectrode topography allows visualization of localized electrochemical reactions with sub-nanoscopic vertical resolution. The PDIM images reported here suggest that in the early stages, Fe dissolution in 0.1 M H_2SO_4 is highly non-uniform, with microscopic surface regions dissolving rapidly within an area that is otherwise stable. The sudden growth and disappearance of shallow pits suggests a model of dissolution whereby the metal corrodes via transient, localized cells.

Acknowledgement. This work was support by the Dept. of Energy/Office of Basic Sciences (DOE/DE-FGO2-88ER45338). The phase detection interferometric microscope was provided by support from the National Science Foundation (CBT-8807676). H.S.W. gratefully acknowledges support provided by the Office of Naval Research Young Investigator Program.

Figures

1. Schematic diagram of the phase-detection interferometric microscope.

2. Voltammogram of 100 μm Fe disk in 0.1 M H_2SO_4. Scan rate = 0.05 V/s.

3. PDIM image of a 100 μm Fe disk electrode sealed in epoxy.

4. Inverted PDIM images of the Fe surface following exposure to 0.1M H_2SO_4. The total exposure time prior to imaging is indicated on the figure. The surface topography has been inverted to allow viewing of pit depth.

5. Profile across Fe surface following exposure to 0.1M H_2SO_4 as a function of time.

6. Profile across Fe surface following exposure to 0.1M H_2SO_4 as a function of time.

References

1. D. M. Perry, P. J. Morgan, and G. M. Robinson, J. Inst. of Electr. and Rad. , 55, 145 (1985).

2. D. M. Perry, G. M. Robinson, and R. W. Peterson, IEEE Trans. on Magnetics, 19, 1656 (1983).

3. G. M. Robinson, C. D. Englund, T. J. Szczech and R. D. Cambronne, ibid, 21,(1985).

4. H.S. White, unpublished results, U. Of Minnesota, 1988.

5. J. F. Biegen and R. A. Smythe, SPIE O/E LASE '88 Sym. on Optoelect. and Laser Appl. in Sci. and Eng., Jan. 1988, Los Angeles, CA.

6. Erik R. Scott and H. S. White, U. Of Minnesota, 1987.

7. R. T. Atanasoski, H. S. White, and W. H. Smyrl, J. Electrochem. Soc., 133, 2435, (1986).

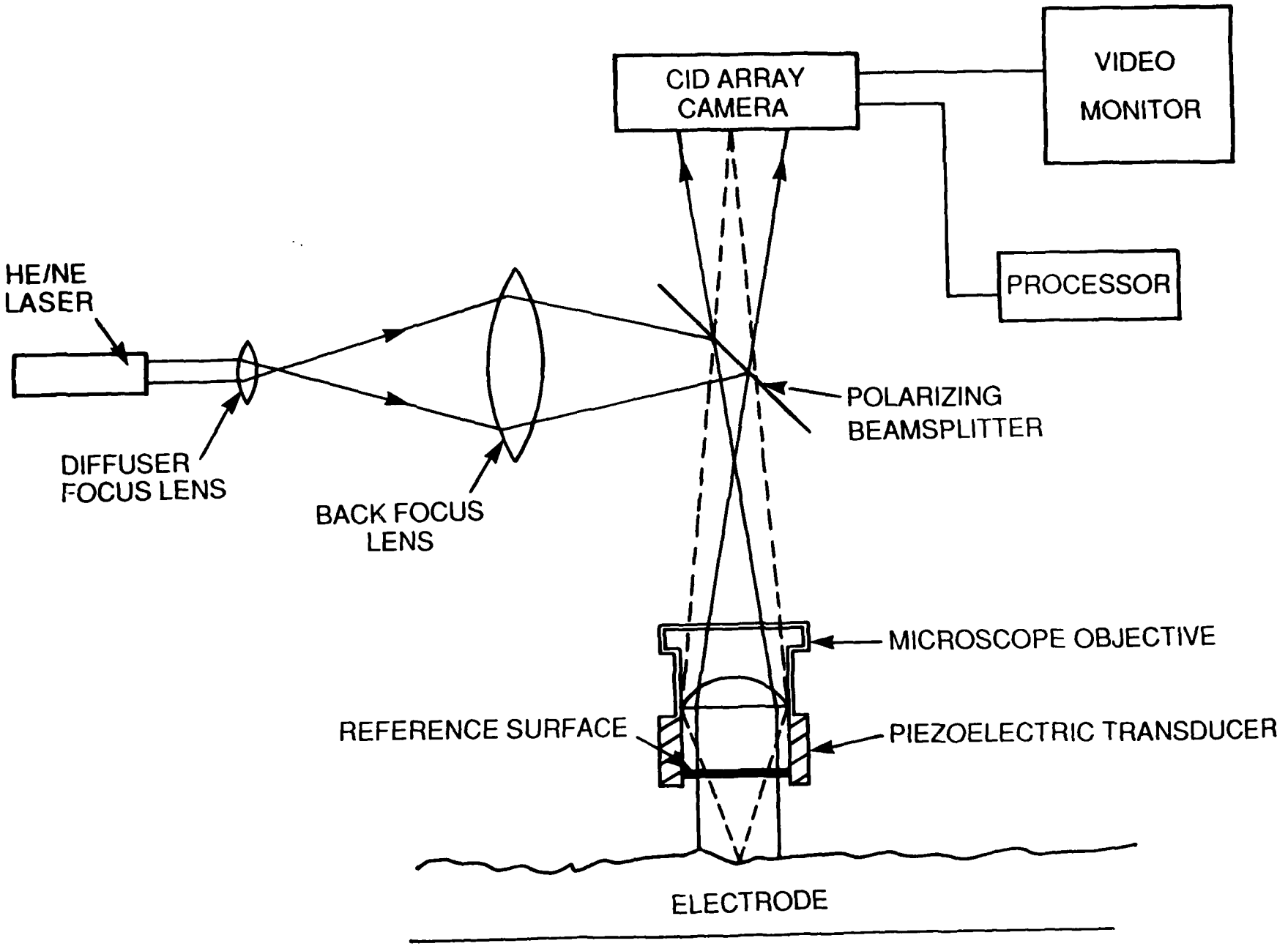
CID ARRAY CAMERA
VIDEO MONITOR
PROCESSOR
HE/NE LASER
DIFFUSER FOCUS LENS
BACK FOCUS LENS
POLARIZING BEAMSPLITTER
MICROSCOPE OBJECTIVE
REFERENCE SURFACE
PIEZOELECTRIC TRANSDUCER
ELECTRODE

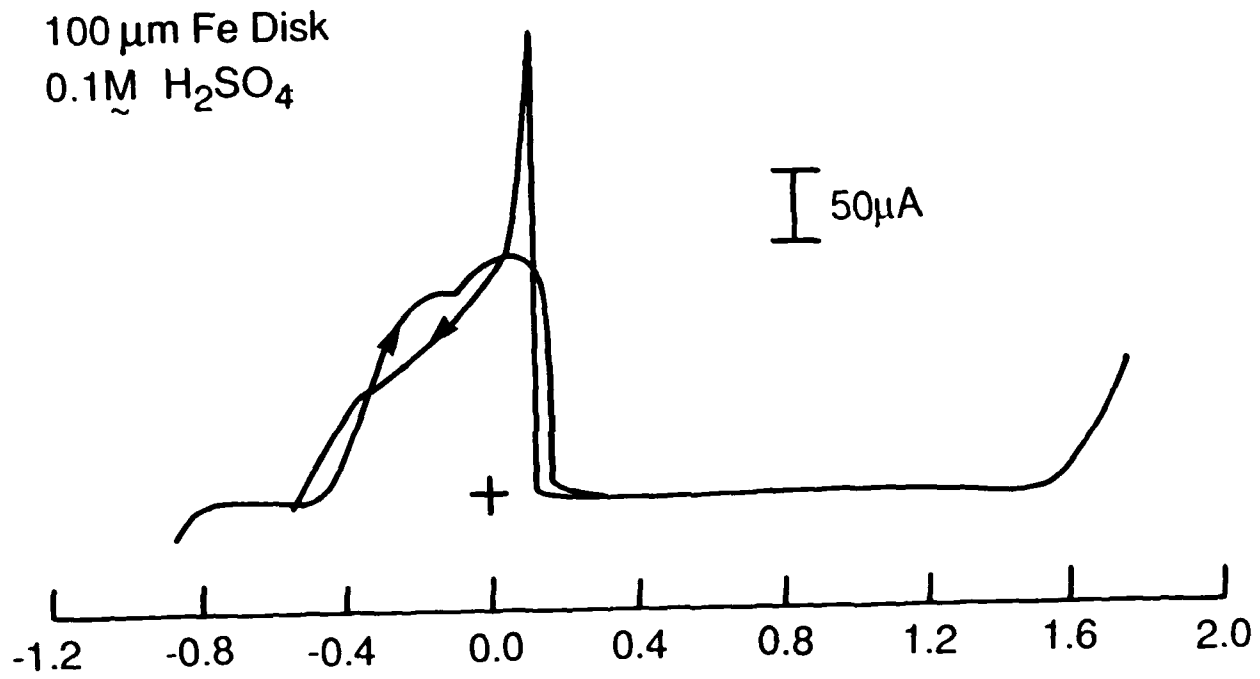
100 µm Fe Disk
0.1M H_2SO_4
50µA
-1.2
-0.8
-0.4
0.0
0.4
0.8
1.2
1.6
2.0
V vs. SSCE

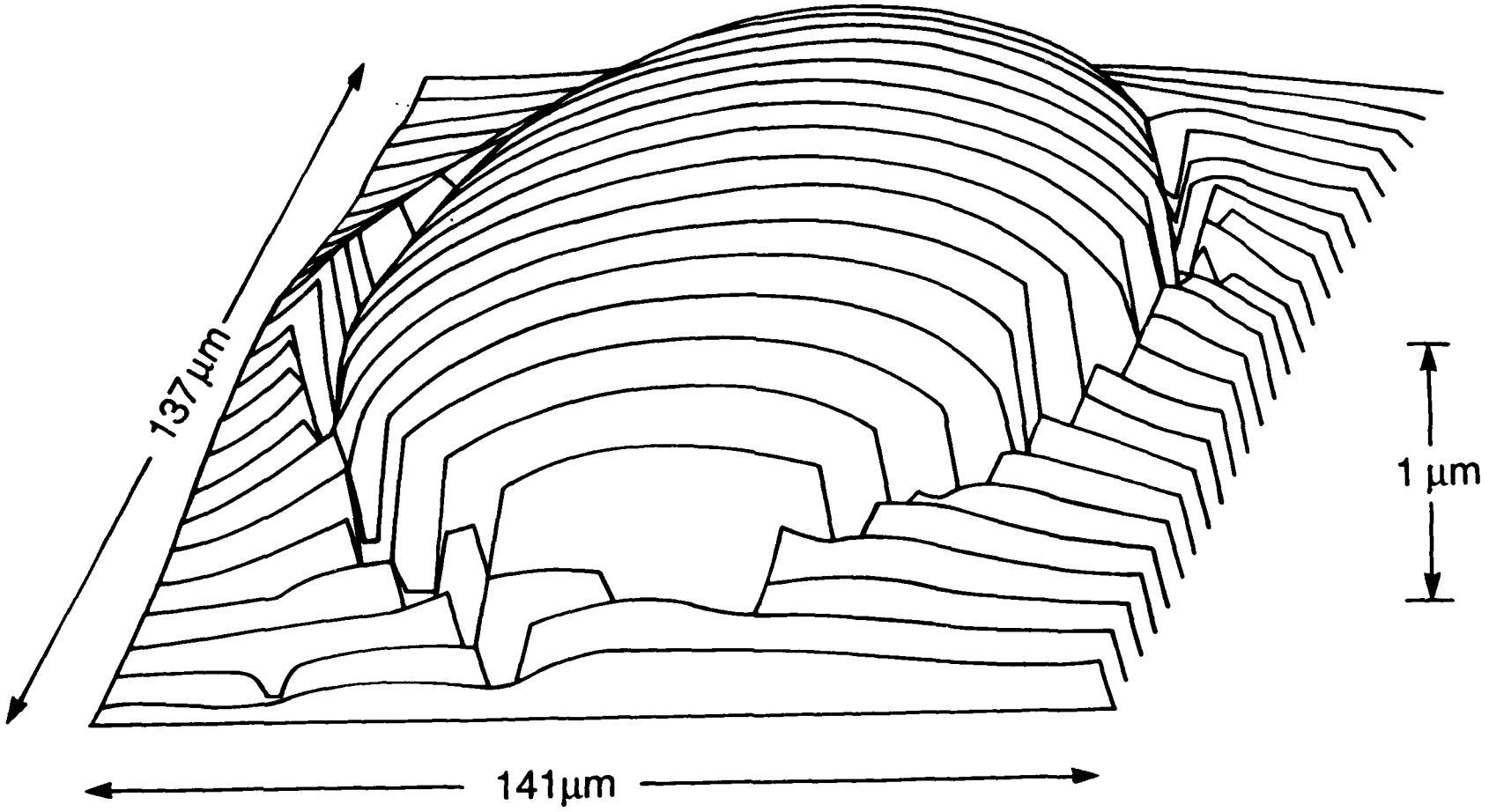
137μm
1 μm
141μm

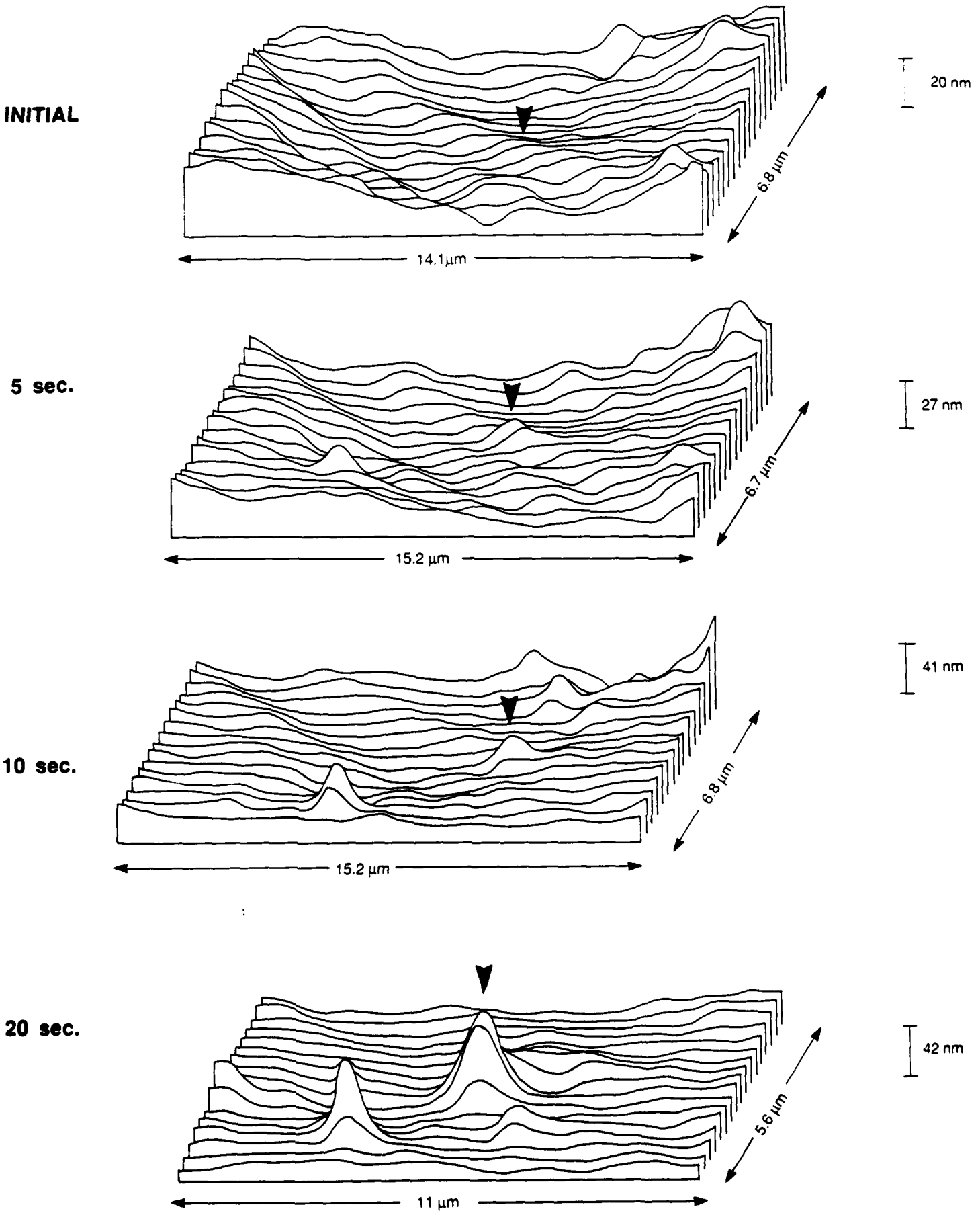
INITIAL
20 nm
6.8 µm
14.1µm
5 sec.
27 nm
6.7 µm
15.2 µm
10 sec.
41 nm
6.8 µm
15.2 µm
20 sec.
42 nm
5.6 µm
11 µm

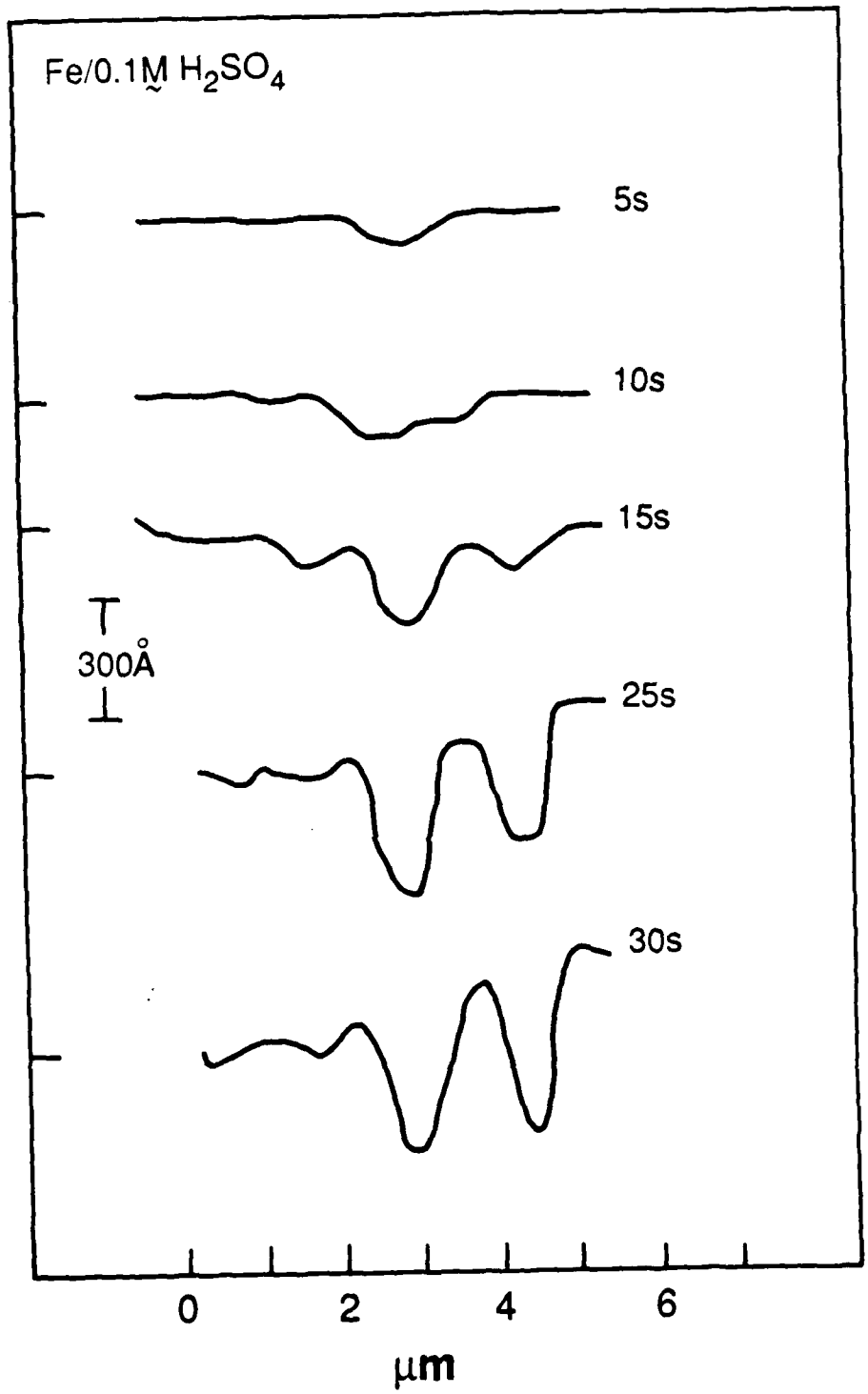
Fe/0.1M H_2SO_4
5s
10s
15s
300Å
25s
30s
0
2
4
6
μm

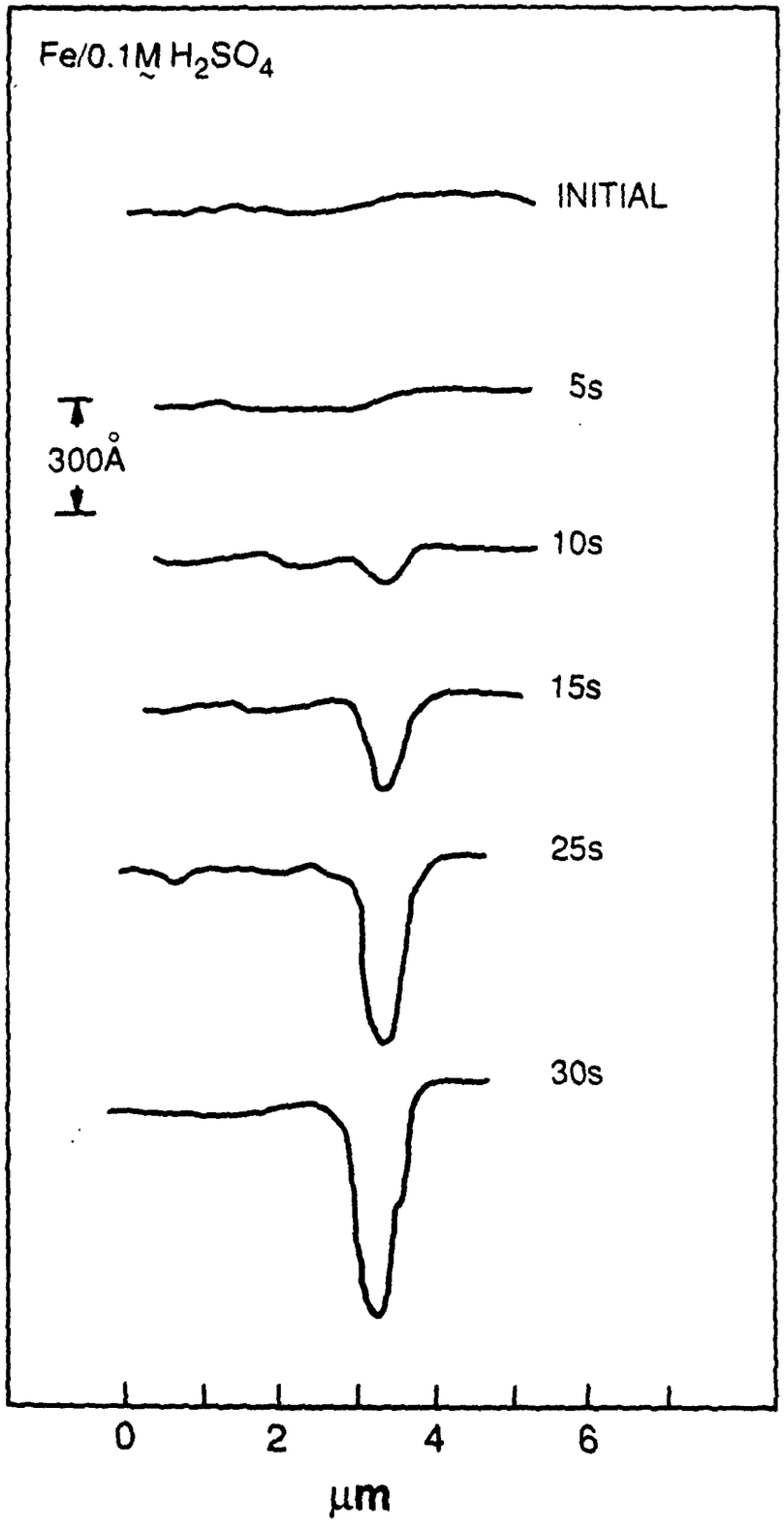
Fe/0.1M H_2SO_4
INITIAL
5s
300Å
10s
15s
25s
30s
0
2
4
6
μm